

Modified Gravitational Theory and Galaxy Rotation Curves

J. W. Moffat

*The Perimeter Institute for Theoretical Physics, Waterloo, Ontario, N2J 2W9,
Canada*

and

Department of Physics, University of Toronto, Toronto, Ontario M5S 1A7, Canada

Abstract

The nonsymmetric gravitational theory predicts an acceleration law that modifies the Newtonian law of attraction between particles. For weak fields a fit to the flat rotation curves of galaxies is obtained in terms of the mass (mass-to-light ratio M/L) of galaxies. The fits assume that the galaxies are not dominated by exotic dark matter. The equations of motion for test particles reduce for weak gravitational fields to the GR equations of motion and the predictions for the solar system and the binary pulsar PSR 1913+16 agree with the observations. The gravitational lensing of clusters of galaxies can be explained without exotic dark matter.

e-mail: jmoffat@perimeterinstitute.ca

1 Introduction

A gravitational theory explanation of the acceleration of the expansion of the universe [1, 2, 3] and the observed flat rotation curves of galaxies was proposed [4], based on the nonsymmetric gravitational theory (NGT) [5, 6, 7]. Since no dark matter has been detected so far, it seems imperative to seek a possible modified gravitational theory that could explain the now large amount of data on galaxy rotation curves. The same holds true for the need to explain the acceleration of the expansion of the universe without having to invoke a cosmological constant, because of the serious problems related to this constant [8].

In the following, we summarize the derivation of the motion of test particles in NGT. We consider the derivation of test particle motion from the NGT conservation laws. The motion of a particle in a static, spherically symmetric gravitational field is derived, yielding the modified Newtonian law of motion for weak gravitational fields. Two parameters $\sqrt{M_0}$ and r_0 occur in the generalized Newtonian acceleration law. The parameter $\sqrt{M_0}$ is modelled for a bound system by a dependence on the mean

orbital radius of a test particle, and the range parameter r_0 is determined for galaxies and clusters of galaxies from the acceleration cH_0 where H_0 is the measured Hubble constant. A fit to both low surface brightness and high surface brightness galaxies is achieved in terms of the total galaxy mass M (or M/L) without exotic dark matter. A satisfactory fit is achieved to the rotational velocity data generic to the elliptical galaxy NGC 3379. Fits to the data of the two spheroidal dwarf galaxies Fornax and Draco and the globular cluster ω Centauri are also obtained. The predicted light bending and lensing can lead to agreement with galaxy cluster lensing observations.

The modelled values of the parameter $\sqrt{M_0}$ for the solar system and Earth, lead to agreement with solar system observations, terrestrial gravitational experiments and the binary pulsar PSR 1913+16 observations.

2 The Field Equations

The nonsymmetric fundamental tensor $g_{\mu\nu}$ is defined by [5, 6, 7]:

$$g_{\mu\nu} = g_{(\mu\nu)} + g_{[\mu\nu]}, \quad (1)$$

where

$$g_{(\mu\nu)} = \frac{1}{2}(g_{\mu\nu} + g_{\nu\mu}), \quad g_{[\mu\nu]} = \frac{1}{2}(g_{\mu\nu} - g_{\nu\mu}). \quad (2)$$

The nonsymmetric connection $\Gamma_{\mu\nu}^\lambda$ is decomposed as

$$\Gamma_{\mu\nu}^\lambda = \Gamma_{(\mu\nu)}^\lambda + \Gamma_{[\mu\nu]}^\lambda. \quad (3)$$

The contravariant tensor $g^{\mu\nu}$ is defined in terms of the equation

$$g^{\mu\nu} g_{\sigma\nu} = g^{\nu\mu} g_{\nu\sigma} = \delta^\mu_\sigma. \quad (4)$$

The NGT action is given by

$$S_{\text{ngt}} = S + S_M, \quad (5)$$

where

$$S = \frac{1}{16\pi G} \int d^4x [\mathbf{g}^{\mu\nu} R_{\mu\nu}^*(W) - 2\Lambda\sqrt{-g} - \frac{1}{4}\mu^2 \mathbf{g}^{\mu\nu} g_{[\nu\mu]}], \quad (6)$$

and S_M is the matter action satisfying the relation

$$\frac{1}{\sqrt{-g}} \left(\frac{\delta S_M}{\delta g^{\mu\nu}} \right) = -\frac{1}{2} T_{\mu\nu}. \quad (7)$$

Here, we have chosen units $c = 1$, $\mathbf{g}^{\mu\nu} = \sqrt{-g} g^{\mu\nu}$, $g = \text{Det}(g_{\mu\nu})$, Λ is the cosmological constant, μ is a mass associated with the skew field $g_{[\mu\nu]}$. Moreover, $T_{\mu\nu}$ is the nonsymmetric energy-momentum tensor and $R_{\mu\nu}^*(W)$ is the tensor

$$R_{\mu\nu}^*(W) = R_{\mu\nu}(W) - \frac{1}{6} W_\mu W_\nu, \quad (8)$$

where $R_{\mu\nu}(W)$ is the NGT contracted curvature tensor

$$R_{\mu\nu}(W) = W_{\mu\nu,\beta}^{\beta} - \frac{1}{2}(W_{\mu\beta,\nu}^{\beta} + W_{\nu\beta,\mu}^{\beta}) - W_{\alpha\nu}^{\beta}W_{\mu\beta}^{\alpha} + W_{\alpha\beta}^{\beta}W_{\mu\nu}^{\alpha}, \quad (9)$$

defined in terms of the unconstrained nonsymmetric connection:

$$W_{\mu\nu}^{\lambda} = \Gamma_{\mu\nu}^{\lambda} - \frac{2}{3}\delta^{\lambda}_{\mu}W_{\nu}, \quad (10)$$

where

$$W_{\mu} = \frac{1}{2}(W_{\mu\lambda}^{\lambda} - W_{\lambda\mu}^{\lambda}). \quad (11)$$

Eq.(10) leads to the result

$$\Gamma_{\mu} = \Gamma_{[\mu\lambda]}^{\lambda} = 0. \quad (12)$$

The contracted tensor $R_{\mu\nu}(W)$ can be written as

$$R_{\mu\nu}(W) = R_{\mu\nu}(\Gamma) + \frac{2}{3}W_{[\mu,\nu]}, \quad (13)$$

where

$$R_{\mu\nu}(\Gamma) = \Gamma_{\mu\nu,\beta}^{\beta} - \frac{1}{2}(\Gamma_{(\mu\beta),\nu}^{\beta} + \Gamma_{(\nu\beta),\mu}^{\beta}) - \Gamma_{\alpha\nu}^{\beta}\Gamma_{\mu\beta}^{\alpha} + \Gamma_{(\alpha\beta)}^{\beta}\Gamma_{\mu\nu}^{\alpha}. \quad (14)$$

The gravitational constant G in the action S is defined in terms of the ‘‘bare’’ gravitational constant G_0 :

$$G = G_0Z, \quad (15)$$

where $G_0 = 6.673 \times 10^{-8} \text{ g}^{-1} \text{ cm}^3 \text{ s}^{-2}$ is Newton’s constant and Z depends on the strength of the coupling of $g_{[\mu\nu]}$ to matter. Thus, $Z = 1$ when $g_{[\mu\nu]}$ is zero and NGT reduces to Einstein’s GR.

A variation of the action S_{ngt} yields the field equations in the presence of matter sources

$$G_{\mu\nu}^*(W) + \Lambda g_{\mu\nu} + S_{\mu\nu} = 8\pi GT_{\mu\nu}, \quad (16)$$

$$\mathbf{g}^{[\mu\nu]}_{,\nu} = -\frac{1}{2}\mathbf{g}^{(\mu\alpha)}W_{\alpha}, \quad (17)$$

$$\begin{aligned} & \mathbf{g}^{\mu\nu}_{,\sigma} + \mathbf{g}^{\rho\nu}W_{\rho\sigma}^{\mu} + \mathbf{g}^{\mu\rho}W_{\sigma\rho}^{\nu} - \mathbf{g}^{\mu\nu}W_{\sigma\rho}^{\rho} \\ & + \frac{2}{3}\delta_{\sigma}^{\nu}\mathbf{g}^{\mu\rho}W_{[\rho\beta]}^{\beta} + \frac{1}{6}(\mathbf{g}^{(\mu\beta)}W_{\beta}\delta_{\sigma}^{\nu} - \mathbf{g}^{(\nu\beta)}W_{\beta}\delta_{\sigma}^{\mu}) = 0. \end{aligned} \quad (18)$$

Here, we have $G_{\mu\nu}^*(W) = R_{\mu\nu}^*(W) - \frac{1}{2}g_{\mu\nu}\mathcal{R}^*(W)$, where $\mathcal{R}^*(W) = g^{\mu\nu}R_{\mu\nu}^*(W)$, and

$$S_{\mu\nu} = \frac{1}{4}\mu^2(g_{[\mu\nu]} + \frac{1}{2}g_{\mu\nu}g^{[\sigma\rho]}g_{[\rho\sigma]} + g^{[\sigma\rho]}g_{\mu\sigma}g_{\rho\nu}). \quad (19)$$

The vacuum field equations in the absence of matter sources are given by

$$R_{\mu\nu}^*(W) = \Lambda g_{\mu\nu} - (S_{\mu\nu} - \frac{1}{2}g_{\mu\nu}\mathcal{S}), \quad (20)$$

where $\mathcal{S} = g^{\mu\nu} S_{\mu\nu}$. For the case of a static, spherically symmetric field with $\mu = 0$ and $g_{[0i]} = 0$ ($i=1,2,3$), the gravitational field is described by the Wyman solution given in Appendix A [9]. In this case the vector $W_\mu = 0$ [4, 6, 7] and the field equations (20) in empty space $T_{\mu\nu} = 0$ become

$$R_{\mu\nu}(\Gamma) = \Lambda g_{\mu\nu} - (S_{\mu\nu} - \frac{1}{2}g_{\mu\nu}\mathcal{S}). \quad (21)$$

The time independent components of these field equations are given in Appendix A.

3 The Equations of Motion of a Particle

In NGT there are two choices for the motion of a particle [10], for there exist two connections, the Christoffel connection given by

$$\left\{ \begin{array}{c} \lambda \\ \mu\nu \end{array} \right\} = \frac{1}{2}s^{(\lambda\rho)} \left(g_{(\mu\rho),\nu} + g_{(\rho\nu),\mu} - g_{(\mu\nu),\rho} \right), \quad (22)$$

where

$$s^{(\nu\alpha)}g_{(\mu\alpha)} = \delta^\nu_\mu, \quad (23)$$

and the nonsymmetric connection $\Gamma_{\mu\nu}^\lambda$. If we define the parallel transport of a vector V^μ by

$$D_\mu V^\lambda = \partial_\mu V^\lambda + \Gamma_{\rho\mu}^\lambda V^\rho, \quad (24)$$

then we obtain the equation of motion

$$u^\nu D_\nu u^\lambda \equiv \frac{du^\lambda}{d\tau} + \Gamma_{\mu\nu}^\lambda u^\mu u^\nu = 0, \quad (25)$$

where τ is the proper time along the path followed by the particle and $u^\lambda = dx^\lambda/d\tau$ is the 4-velocity of the particle. This defines the path equation which is not a path of extremal length.

We can derive the second equation of motion by using the Lagrangian defined by

$$L = g_{(\mu\nu)}u^\mu u^\nu. \quad (26)$$

We have

$$\frac{1}{2} \left(\frac{d}{d\tau} \frac{\partial L}{\partial u^\alpha} - \frac{\partial L}{\partial x^\alpha} \right) = g_{(\mu\nu)}u^\mu u^\nu \left(\left\{ \begin{array}{c} \beta \\ \mu\nu \end{array} \right\} - \Gamma_{\mu\nu}^\beta \right). \quad (27)$$

We see that when the right-hand side vanishes, the Euler-Lagrangian equations are satisfied and we get the extremal geodesic equation

$$\frac{du^\mu}{d\tau} + \left\{ \begin{array}{c} \mu \\ \alpha\beta \end{array} \right\} u^\alpha u^\beta = 0. \quad (28)$$

The conservation laws in NGT can be written [11]:

$$\partial_\rho \tilde{\mathbf{T}}_\lambda^\rho - \frac{1}{2} \partial_\lambda g_{\mu\nu} \mathbf{T}^{\mu\nu} = 0, \quad (29)$$

where

$$\tilde{\mathbf{T}}_\lambda^\rho = \frac{1}{2} (g_{\mu\lambda} \mathbf{T}^{\mu\rho} + g_{\lambda\mu} \mathbf{T}^{\rho\mu}). \quad (30)$$

Let us assume a monopole test particle

$$\int d^3x \mathbf{T}^{\mu\nu} \neq 0, \quad (31)$$

$$\int d^3x (x^\alpha - X^\alpha) \mathbf{T}^{\mu\nu} = 0, \quad (32)$$

and similarly for higher moments. The integration is carried out over a hypersurface of constant t , following the procedure of Papapetrou [12], and X^α is the position of the monopole. It can be shown that (29) leads to

$$\begin{aligned} & \frac{d}{dt} \left(\frac{dX^\beta}{dt} \int d^3x \mathbf{t}^{00} \right) + \left\{ \begin{matrix} \beta \\ \mu\nu \end{matrix} \right\} \frac{dX^\mu}{dt} \frac{dX^\nu}{dt} \int d^3x \mathbf{t}^{00} \\ &= \frac{1}{2} s^{(\lambda\beta)} \left(\partial_\lambda g_{\mu\nu} \int d^3x \mathbf{T}^{\mu\nu} - \partial_\lambda g_{(\mu\nu)} \frac{dX^\mu}{dt} \frac{dX^\nu}{dt} \int d^3x \mathbf{t}^{00} \right), \end{aligned} \quad (33)$$

where $\mathbf{t}^{\mu\nu} = s^{(\lambda\nu)} \tilde{\mathbf{T}}_\lambda^\mu$. If we assume that $\mathbf{T}^{[\mu\nu]} = 0$, then we get

$$\frac{d}{d\tau} \left(m \frac{dX^\beta}{d\tau} \right) + m \left\{ \begin{matrix} \beta \\ \mu\nu \end{matrix} \right\} \frac{dX^\mu}{d\tau} \frac{dX^\nu}{d\tau} = 0, \quad (34)$$

where

$$m = \frac{d\tau}{dt} \int d^3x \mathbf{t}^{00}. \quad (35)$$

This leads us to the geodesic equation (28). However, we cannot in general assume that $T^{[\mu\nu]}$ is zero, for it is associated with the intrinsic spin of matter or to the skew field $g_{[\mu\nu]}$ itself, and we must include a coupling to the spin and skew field on the right-hand side of (34). We shall find that in the weak field approximation the path equation (25) and the geodesic equation (28) become approximately the same, including a necessary coupling to a skew symmetric source.

4 Particle Motion in a Static Spherically Symmetric Gravitational Field

It was shown in ref. [10] that for large values of r in the static, spherically symmetric solution of the NGT field equations, *the geodesic equation and the path equation yield similar physical results*. Since we shall be concerned with the dynamics of galaxies,

we shall treat the case of the geodesic equation coupled to a skew symmetric source. We have

$$\frac{du^\beta}{d\tau} + \left\{ \begin{matrix} \beta \\ \mu\nu \end{matrix} \right\} u^\mu u^\nu = s^{(\beta\alpha)} f_{[\alpha\mu]} u^\mu, \quad (36)$$

where

$$f_{[\alpha\mu]} = \lambda \partial_{[\alpha} \left(\frac{\epsilon^{\eta\sigma\nu\lambda}}{\sqrt{-g}} H_{[\sigma\nu\lambda]} g_{(\mu)\eta} \right). \quad (37)$$

Here, the skew tensor $\epsilon^{\mu\nu\lambda\eta}$ is the Levi-Civita tensor density and $H_{[\mu\nu\lambda]}$ is given by

$$H_{[\mu\nu\lambda]} = \frac{1}{3} (\partial_\lambda g_{[\mu\nu]} + \partial_\mu g_{[\nu\lambda]} + \partial_\nu g_{[\lambda\mu]}), \quad (38)$$

and λ is a coupling constant with the dimension of length that couples the skew field to the test particle.

In the static, spherically symmetric field of NGT, the tensor $H_{[\mu\nu\lambda]}$ has only one non-vanishing component

$$H_{[\theta\phi r]} = \frac{1}{3} \partial_r g_{[\theta\phi]} = f' \sin \theta \quad (39)$$

and we get

$$f_{[r0]} = \lambda \frac{d}{dr} \left(\frac{\gamma f'}{\sqrt{\alpha\gamma(r^4 + f^2)}} \right). \quad (40)$$

The equations of motion for a test particle are given by

$$\begin{aligned} \frac{d^2 r}{d\tau^2} + \frac{\alpha'}{2\alpha} \left(\frac{dr}{d\tau} \right)^2 - \frac{r}{\alpha} \left(\frac{d\theta}{d\tau} \right)^2 - r \left(\frac{\sin^2 \theta}{\alpha} \right) \left(\frac{d\phi}{d\tau} \right)^2 + \frac{\gamma'}{2\alpha} \left(\frac{dt}{d\tau} \right)^2 \\ + \frac{d}{dr} \left(\frac{\lambda\gamma f'}{\sqrt{\alpha\gamma(r^4 + f^2)}} \right) \left(\frac{dt}{d\tau} \right) = 0, \end{aligned} \quad (41)$$

$$\frac{d^2 t}{d\tau^2} + \frac{\gamma'}{\gamma} \left(\frac{dt}{d\tau} \right) \left(\frac{dr}{d\tau} \right) + \frac{1}{\gamma} \frac{d}{dr} \left(\frac{\lambda\gamma f'}{\sqrt{\alpha\gamma(r^4 + f^2)}} \right) = 0, \quad (42)$$

$$\frac{d^2 \theta}{d\tau^2} + \frac{2}{r} \left(\frac{d\theta}{d\tau} \right) \left(\frac{dr}{d\tau} \right) - \sin \theta \cos \theta \left(\frac{d\phi}{d\tau} \right)^2 = 0, \quad (43)$$

$$\frac{d^2 \phi}{d\tau^2} + \frac{2}{r} \left(\frac{d\phi}{d\tau} \right) \left(\frac{dr}{d\tau} \right) + 2 \cot \theta \left(\frac{d\phi}{d\tau} \right) \left(\frac{d\theta}{d\tau} \right) = 0. \quad (44)$$

The orbit of the test particle can be shown to lie in a plane and by an appropriate choice of axes, we can make $\theta = \pi/2$. Integrating Eq.(44) gives

$$r^2 \frac{d\phi}{d\tau} = J, \quad (45)$$

where J is the conserved orbital angular momentum. Integration of Eq.(42) gives

$$\frac{dt}{d\tau} = -\frac{1}{\gamma} \left[\frac{\lambda\gamma f'}{\sqrt{\alpha\gamma(r^4 + f^2)}} + E \right], \quad (46)$$

where E is the constant energy per unit mass.

By substituting (46) into (41) and using (45), we obtain

$$\frac{d^2r}{d\tau^2} + \frac{\alpha'}{2\alpha} \left(\frac{dr}{d\tau} \right)^2 - \frac{J^2}{\alpha r^3} + \frac{\gamma'}{2\alpha\gamma^2} \left[\frac{\lambda\gamma f'}{\sqrt{\alpha\gamma(r^4 + f^2)}} + E \right]^2 = \frac{1}{\gamma} \frac{d}{dr} \left[\frac{\lambda\gamma f'}{\sqrt{\alpha\gamma(r^4 + f^2)}} + E \right]. \quad (47)$$

Let us now make the approximations that $\lambda f'/r^2 \ll 1$, $f/r^2 \ll 1$ and the slow motion approximation $dr/dt \ll 1$. Then, for material particles we set $E = 1$ and (47) becomes

$$\frac{d^2r}{dt^2} - \frac{J_N^2}{r^3} + \frac{GM}{r^2} = \lambda \frac{d}{dr} \left(\frac{f'}{r^2} \right), \quad (48)$$

where J_N is the Newtonian orbital angular momentum.

5 Linear Weak Field Approximation

We expand $g_{\mu\nu}$ about a Ricci-flat GR background

$$g_{\mu\nu} = g_{(\mu\nu)}^{GR} + h_{\mu\nu} + O(h^2), \quad (49)$$

where $g_{(\mu\nu)}^{GR}$ is the GR background metric. The skew field $h_{[\mu\nu]}$ obeys the linearized equation of motion in the GR background geometry

$$\nabla^\sigma F_{\mu\nu\sigma} + 4h^{[\sigma\beta]} B_{\beta\mu\sigma\nu} + \mu^2 h_{[\mu\nu]} = 0, \quad (50)$$

where

$$F_{[\mu\nu\lambda]} = \partial_\lambda h_{[\mu\nu]} + \partial_\mu h_{[\nu\lambda]} + \partial_\nu h_{[\lambda\mu]} \quad (51)$$

and ∇^λ and $B_{\beta\mu\sigma\nu}$ denote the background GR covariant derivative and curvature tensor, respectively. Moreover,

$$W_\mu = -2\nabla^\lambda h_{[\mu\lambda]}. \quad (52)$$

For flat Minkowski spacetime, Eq.(50) reduces exactly to the massive Kalb-Ramond-Proca equation [13], which is free of ghost pole instabilities with a positive Hamiltonian bounded from below.

For the static, spherically symmetric spacetime, the linearized equation of motion (50) on a Schwarzschild background takes the form

$$\left(1 - \frac{2GM}{r} \right) f'' - \frac{2}{r} \left(1 - \frac{3GM}{r} \right) f' - \left(\mu^2 + \frac{8GM}{r^3} \right) f = 0, \quad (53)$$

where we assume that $\gamma(r) \sim 1/\alpha(r) \sim 1 - 2GM/r$ and $\beta(r) = r^2$. The solution to this equation in leading order is [6, 14, 15]

$$f(r) = \frac{sG^2M^2}{3} \frac{\exp(-\mu r)}{(\mu r)^{\mu GM}} \left(1 + \mu r + \frac{GM}{r} \left[2 + \mu r \exp(2\mu r) Ei(1, 2\mu r)(\mu r - 1) \right] \right), \quad (54)$$

where Ei is the exponential integral function

$$Ei(n, x) = \int_1^\infty dt \frac{\exp(-xt)}{t^n}. \quad (55)$$

The constant $sG^2M^2/3$ is fixed from the exact Wyman solution with $A = 0$ by taking the limit $\mu \rightarrow 0$.

For large r we obtain

$$f(r) = \frac{1}{3} \frac{sG^2M^2 \exp(-\mu r)(1 + \mu r)}{(\mu r)^{\mu M}}, \quad (56)$$

and for $\mu GM \ll 1$, we have $(\mu r)^{\mu GM} \sim 1$, giving

$$f(r) = \frac{1}{3} sG^2M^2 \exp(-\mu r)(1 + \mu r). \quad (57)$$

This is a solution to the equation

$$f''(r) - \frac{2}{r} f'(r) - \mu^2 f(r) = 0. \quad (58)$$

If we consider the expansion about a GR Schwarzschild background, then (58) is valid for $\mu^2 \gg 8GM/r^3$.

To the order of weak field approximation, we obtain from Eq.(48):

$$\frac{d^2r}{dt^2} - \frac{J_N^2}{r^3} = -\frac{GM}{r^2} + \frac{\sigma \exp(-\mu r)}{r^2} (1 + \mu r), \quad (59)$$

where the constant σ is given by

$$\sigma = \frac{\lambda s G^2 M^2 \mu^2}{3}. \quad (60)$$

Here, λ and s denote the coupling strengths of the test particle and the skew $g_{[23]}$ field, respectively. In Eq. (59), we have required that the additional NGT acceleration on the right-hand side is a repulsive force. This is in keeping with the weak field approximation result obtained in [5, 6], which corresponds to a skew force produced by a massive axial vector spin 1^+ boson exchange.

6 Orbital Equation of Motion

Let us write the line element as

$$ds^2 = \gamma dt^2 - \alpha dr^2 - r^2(d\theta^2 + \sin^2 \theta d\phi^2). \quad (61)$$

We set $\theta = \pi/2$ and divide the resulting expression by $d\tau^2$ and use Eqs.(45) and (46) to obtain

$$\left(\frac{dr}{d\tau}\right)^2 + \frac{J^2}{\alpha r^2} - \frac{1}{\alpha\gamma} \left[\frac{\lambda\gamma f'}{\sqrt{\alpha\gamma(r^4 + f^2)}} + E \right]^2 = -\frac{E}{\alpha}. \quad (62)$$

We have $ds^2 = Ed\tau^2$, so that $ds/d\tau$ is a constant. For material particles $E > 0$ and for massless photons $E = 0$.

Let us set $u = 1/r$ and by using (45), we have $dr/d\tau = -Jdu/d\phi$. Substituting this into (62), we obtain

$$\left(\frac{du}{d\phi}\right)^2 = \frac{1}{\alpha\gamma J^2} \left[E + \frac{\lambda\gamma f'}{\sqrt{\alpha\gamma(r^4 + f^2)}} \right]^2 - \frac{1}{\alpha r^2} - \frac{E}{\alpha J^2}. \quad (63)$$

By substituting $dr/d\phi = -(1/u^2)du/d\phi$ into (63) and using the approximation $\gamma \sim 1/\alpha \sim 1 - 2GM/r$ and $f/r^2 \ll 1$ and $\lambda f'/r^2 \ll 1$, we get after some manipulation

$$\frac{d^2u}{d\phi^2} + u = \frac{EGM}{J^2} - \frac{E\lambda s G^2 M^2}{3r_0^2 J^2} \exp\left(-\frac{1}{r_0 u}\right) \left(1 + \frac{1}{r_0 u}\right) + 3GMu^2, \quad (64)$$

where $r_0 = 1/\mu$.

For material test particles $E = 1$ and we obtain

$$\frac{d^2u}{d\phi^2} + u = \frac{GM}{J^2} + 3GMu^2 - \frac{K}{J^2} \exp\left(-\frac{1}{r_0 u}\right) \left(1 + \frac{1}{r_0 u}\right), \quad (65)$$

where $K = \lambda s G^2 M^2 / 3r_0^2$. On the other hand, for massless photons $ds^2 = 0$ and $E = 0$ and (64) gives

$$\frac{d^2u}{d\phi^2} + u = 3GMu^2. \quad (66)$$

7 Galaxy Rotational Velocity Curves

A possible explanation of the galactic rotational velocity curves problem has been obtained in NGT [16]. From the radial acceleration derived from (59) experienced by a test particle in a static, spherically symmetric gravitational field due to a point source, we obtain

$$a(r) = -\frac{G_\infty M}{r^2} + \sigma \frac{\exp(-r/r_0)}{r^2} \left(1 + \frac{r}{r_0}\right), \quad (67)$$

Moreover, $G \equiv G_\infty$ is defined to be the gravitational constant at infinity

$$G_\infty = G_0 \left(1 + \sqrt{\frac{M_0}{M}} \right), \quad (68)$$

where G_0 is Newton's "bare" gravitational constant. This conforms with our definition of G in Eq.(15), which requires that G be renormalized in order to guarantee that (67) reduces to the Newtonian acceleration

$$a_{\text{Newton}} = -\frac{G_0 M}{r^2} \quad (69)$$

at small distances $r \ll r_0$. The constant σ is given by

$$\sigma = \frac{\lambda s G_0^2 M^2}{3c^2 r_0^2}. \quad (70)$$

The integration constant s in (70), occurring in the static, spherically symmetric solution (see, Appendix A), is dimensionless and can be modelled as

$$s = gM^a, \quad (71)$$

where M is the total mass of the particle source, g is a coupling constant and a is a dimensionless constant. We choose $a = -3/2$ and $\lambda g G_0^2 / 3c^2 r_0^2 = G_0 \sqrt{M_0}$ where M_0 is a parameter. The choice of $a = -3/2$ yields for a galaxy dynamics the Tully-Fisher law [19].

We obtain the acceleration on a point particle

$$a(r) = -\frac{G_\infty M}{r^2} + G_0 \sqrt{MM_0} \frac{\exp(-r/r_0)}{r^2} \left(1 + \frac{r}{r_0} \right). \quad (72)$$

By using (68), we can write the NGT acceleration in the form

$$a(r) = -\frac{G_0 M}{r^2} \left\{ 1 + \sqrt{\frac{M_0}{M}} \left[1 - \exp(-r/r_0) \left(1 + \frac{r}{r_0} \right) \right] \right\}. \quad (73)$$

We conclude that the gravitational constant can be different at small and large distance scales depending on the size of the parameter $\sqrt{M_0}$. We have two parameters: the parameter $\sqrt{M_0}$ and the distance range r_0 . We assume that G_∞ scales for constant M with increasing strength as $\sqrt{M_0}$, while for fixed values of M_0 we have $G_\infty \rightarrow G_0$ as the total mass of the source $M \rightarrow \infty$. Let us model the parameter $\alpha = \sqrt{M_0}$ as a function of the mean orbital radius of a test particle

$$\alpha \equiv \sqrt{M_0} = k \langle r_{\text{orb}} \rangle^n, \quad (74)$$

where k and n are constants. We shall choose the exponent to be $n = 3/2$. We shall apply (73) to explain the flatness of rotation curves of galaxies, as well as the

approximate Tully-Fisher law [19], $G_0 M \sim v^4$, where v is the rotational velocity of a galaxy and M is the galaxy mass

$$M = M_* + M_{HI} + M_{DB} + M_f. \quad (75)$$

Here, M_* , M_{HI} , M_{DB} and M_f denote the visible mass, the mass of neutral hydrogen, possible dark baryon mass and gas, and the mass from the skew field energy density, respectively. In [4], we obtained from the modified Friedmann equations

$$\Omega = \Omega_b + \Omega_m + \Omega_f, \quad (76)$$

where Ω_b , Ω_m and Ω_f denote the fractional values of baryons, $g_{[\mu\nu]}$ field matter density and smooth $g_{[\mu\nu]}^0$ field density background, respectively, obtained from the expansion

$$g_{[\mu\nu]} = g_{[\mu\nu]}^0 + \delta g_{[\mu\nu]}, \quad (77)$$

where the smooth background $g_{[\mu\nu]}^0$ and the fluctuations $\delta g_{[\mu\nu]}$ describe the “dark energy” and “dark matter” components, respectively. The NGT cosmological field equations must be solved to yield the observational results $\Omega_b \sim 0.05$, $\Omega_m \sim 0.3$, and $\Omega \sim 0.7$ in order to be consistent with WMAP and supernovae data [1, 2, 3]. The quantities Ω_m and Ω_f in NGT replace the dark matter and dark energy. The mass M_f obtained from the skew field density ρ_m is expected to contribute to the total mass M of galaxies.

The rotational velocity of a star v is given by

$$v = \sqrt{\frac{G_0 M}{r}} \left\{ 1 + \sqrt{\frac{M_0}{M}} \left[1 - \exp(-r/r_0) \left(1 + \frac{r}{r_0} \right) \right] \right\}^{1/2}. \quad (78)$$

Let us postulate that the parameters M_0 and r_0 give the magnitude of the constant acceleration

$$a_0 = \frac{G_0 M_0}{r_0^2}. \quad (79)$$

We assume that for galaxies and clusters of galaxies this acceleration is determined by

$$a_0 = c H_0. \quad (80)$$

Here, H_0 is the current measured Hubble constant $H_0 = 100 h \text{ km s}^{-1} \text{ Mpc}^{-1}$ where $h = (0.71 \pm 0.07)$ [17]. This gives

$$a_0 = 6.90 \times 10^{-8} \text{ cm s}^{-2}. \quad (81)$$

A good fit to low surface brightness and high surface brightness galaxy data is obtained with the parameters

$$M_0 = 9.60 \times 10^{11} M_\odot, \quad r_0 = 13.92 \text{ kpc} = 4.30 \times 10^{22} \text{ cm} \quad (82)$$

and M (or the mass-to-light ratio M/L). Substituting $M_0 = 9.60 \times 10^{11} M_\odot$ into (79) yields the r_0 in (82). Thus, we fit the galaxy rotation curve data with one parameter M_0 and the total galaxy mass M . Since we are using an equation of motion for point particle sources, we are unable to fit the cores of galaxies. A possible model for the galaxy cores is to assume for a radius $r \ll r_c$, where r_c is the core radius, a rotation curve of an isothermal sphere in the ideal case where we can consider a massless disk embedded in it. Then, for $r \ll r_c$:

$$v(r) \sim \left(\frac{4\pi G_0 \rho_c}{3} \right)^{1/2} r, \quad (83)$$

where ρ_c is the core density. For $r \gg r_c$, the rotational velocity curve will be described by the NGT model (78). Further investigation of this issue will require solving the field equations of NGT for a core mass density profile and will be the subject of future research.

We can now fix the constant k in Eq.(74) by using the relation

$$k = \frac{\alpha_g}{\langle r_{\text{orb}} \rangle_g^{3/2}}, \quad (84)$$

where α_g and $\langle r_{\text{orb}} \rangle_g$ denote the values of these quantities for galaxies, respectively. For the mean value $\langle r_{\text{orb}} \rangle_g$ we choose

$$\langle r_{\text{orb}} \rangle_g = 200 \text{ kpc} \quad (85)$$

and using the value of M_0 in (82) we obtain

$$k = 2.02 \times 10^{-13} \text{ g}^{1/2} \text{ cm}^{-1}. \quad (86)$$

The fits to the galaxy rotation curves v in km/s versus the galaxy radius r in kpc are shown in Fig. 1. The data are obtained from ref. [18].

In Fig. 2, fits to two dwarf galaxies (dSph) are shown. We assume that the relation between the velocity dispersion σ and the rotational velocity v takes the simple form in e.g. an isothermal sphere model for which $v \sim \sqrt{2}\sigma$. The error bars on the data [20] for the velocity dispersions are large, and in the case of Draco, due to the small radial range $0.1 \text{ kpc} < r < 0.6 \text{ kpc}$, the Newtonian curve for

$$v = \sqrt{\frac{G_0 M}{r}}, \quad (87)$$

cannot be distinguished within the errors from the NGT prediction. However, it is noted that the NGT prediction for v appears to flatten out as r increases. For Draco $M/L = 28.93 + 50.30(9.58)(M_\odot/L_\odot)$, whereas for Fornax $M/L = 1.79 + 0.72(0.40)(M_\odot/L_\odot)$. There is also an expected large error in the distance estimates to the dSph. Another serious potential source of error is that it is assumed that dSph galaxies are in dynamical equilibrium. The two studied here are members of

the Local Group and exist in the gravitational field of a larger galaxy, the Milky Way. Thus, the tidal interactions with the larger galaxy are expected to affect the dynamics of dSph galaxies and the interpretations of velocity dispersions [21]. These issues and others for dSph galaxies are critically considered in the context of dark matter models by Kormendy and Freeman [22].

We have also included a fit to the elliptical galaxy NGC 3379. The elliptical galaxy NGC 3379 has been the source of controversy recently [23]. The velocities of elliptical galaxies are randomly distributed in the galaxy. However, the gravitational potential that would be experienced by a test particle star or planetary nebula in circular rotation about the center of the galaxy can be extracted from the line-of-sight velocity dispersion profiles. The data for $R/R_{\text{eff}} > 0.5$ refer to planetary nebula.

We use the mean values of the extracted rotational velocities for NGC 3379, obtained by Romanowsky et al. [23] and find that the NGT predicted rotational velocities agree well with their data. According to Romanowsky et al. there appears to be a dearth of dark matter in the elliptical galaxy which needs to be explained by dark matter models and N-body cosmological simulations. For Milgrom’s MOND [24, 25] it is argued by Sanders and Milgrom [26] that NGC 3379 is marginally within the MOND regime with an acceleration $a \sim (a_0)_{\text{Milgrom}} \sim 1.2 \times 10^{-8} \text{ cm s}^{-2}$, so MOND should not apply to the elliptical galaxies. As we see from the fit to the data, the NGT results agree well with the data. Romanowsky et al. also give data for the two elliptical galaxies NGC 821 and NGC 4494, but the intrinsic circular velocities associated with the line-of-sight velocity dispersion profile data are not given by the authors, although the trends of the data are similar to NGC 3379.

A fit to the data for the globular cluster ω Centauri is shown in Fig. 3. The data is from McLaughlin and Meylan [27]. We use the velocity dispersion data and assume that the data is close to the rotational velocity curves associated with the velocity dispersion σ_p i.e. the isothermal sphere model relation $v \sim \sqrt{2}\sigma_p$ holds. The fit to the data reveals that the predicted rotational velocity cannot be distinguished from the Newtonian-Kepler circular velocity curve within the orbital radius of the data. The authors conclude that there appears to be no room for Milgrom’s MOND or dark matter, whereas the NGT results agree well with the data.

In Fig.4, we display a 3-dimensional plot of v versus the range of distance $0.1 \text{ kpc} < r < 10 \text{ kpc}$ and the range of total galaxy mass M used in the fitting of rotational velocity data. The red surface shows the Newtonian values of the rotational velocity v , while the black surface displays the NGT prediction for v .

Table 1, displays the values of the total mass M used to fit the galaxies and the mass-to-light ratios M/L estimated from the data in references given in [18].

There are now about 100 galaxies with available rotational velocity data [18]. However, some of these galaxies are not well described by spherically symmetric halos or have some other disturbing physical feature, so we are unable to obtain fits to these data.

In Milgrom's phenomenological model [24, 25] we have

$$v^4 = G_0 M (a_0)_{\text{Milgrom}}, \quad (88)$$

where

$$(a_0)_{\text{Milgrom}} = 1.2 \times 10^{-8} \text{ cm s}^{-2}. \quad (89)$$

We see that (88) predicts that the rotational velocity is constant out to an infinite range and the rotational velocity does not depend on a distance scale, but on the magnitude of the acceleration $(a_0)_{\text{Milgrom}}$. In contrast, the NGT acceleration formula does depend on the radius r and the distance scale r_0 which for galaxies is fixed by the formula (80).

8 Local and Solar System Observations

We obtain from Eq.(65) the orbit equation

$$\frac{d^2 u}{d\phi^2} + u = \frac{GM}{c^2 J^2} - \frac{K}{J^2} \exp(-r/r_0) \left[1 + \left(\frac{r}{r_0} \right) \right] + \frac{3GM}{c^2} u^2, \quad (90)$$

where now $K = \lambda s G^2 M^2 / 3c^4 r_0^2$. Using the large r weak field approximation, and the expansion

$$\exp(-r/r_0) = 1 - \frac{r}{r_0} + \frac{1}{2} \left(\frac{r}{r_0} \right)^2 + \dots \quad (91)$$

we obtain the orbit equation for $r < r_0$:

$$\frac{d^2 u}{d\phi^2} + u = \frac{GM}{c^2 J_N^2} - \frac{K}{J_N^2} + 3 \frac{GM}{c^2} u^2. \quad (92)$$

We can write this as

$$\frac{d^2 u}{d\phi^2} + u = N + 3 \frac{GM}{c^2} u^2, \quad (93)$$

where

$$N = \frac{GM}{c^2 J_N^2} - \frac{K}{J_N^2}. \quad (94)$$

We can solve Eq.(93) by perturbation theory and find for the perihelion advance of a planetary orbit

$$\Delta\omega = \frac{6\pi}{c^2 p} (GM_\odot - c^2 K_\odot), \quad (95)$$

where $J_N = (GM_\odot p / c^2)^{1/2}$, $p = a(1 - e^2)$ and a and e denote the semimajor axis and the eccentricity of the planetary orbit, respectively.

We choose for the mean orbital radius of the solar planetary system

$$\langle r_{\text{orb}} \rangle_\odot = 1 \text{ a.u.} = 1.49 \times 10^{13} \text{ cm}, \quad (96)$$

which yields using (74) and $k = 2 \times 10^{-13} \text{ g}^{1/2} \text{ cm}^{-1}$:

$$\alpha_{\odot} \equiv (\sqrt{M_0})_{\odot} = 1.2 \times 10^7 \text{ g}^{1/2} \quad (97)$$

and

$$\left(\sqrt{\frac{M_0}{M}}\right)_{\odot} = 2.6 \times 10^{-10}. \quad (98)$$

This result gives

$$\frac{\Delta G}{G_0} \sim 10^{-10}. \quad (99)$$

and $G = G_0$ within the experimental errors for the measurement of Newton's constant G_0 .

We choose for the solar system $K_{\odot} \ll 1.5 \text{ km}$ and use $G = G_{\infty} = G_0$ to obtain from (95) a perihelion advance of Mercury in agreement with GR.

For terrestrial experiments and orbits of satellites, we choose the mean orbital radius equal to the earth-moon distance, $\langle r_{\text{orb}} \rangle_{\oplus} = 3.57 \times 10^{10} \text{ cm}$, which gives

$$\left(\sqrt{\frac{M_0}{M}}\right)_{\oplus} = 1.7 \times 10^{-11}. \quad (100)$$

This also yields $G = G_0$ within the experimental errors.

For the binary pulsar PSR 1913+16 the formula (95) can be adapted to the periastron shift of a binary system. Combining this with the NGT gravitational wave radiation formula, which will approximate closely the GR formula, we can obtain agreement with the observations for the binary pulsar. We choose the mean orbital radius equal to the projected semi-major axis of the binary, $\langle r_{\text{orb}} \rangle_N = 7 \times 10^{10} \text{ cm}$, giving $(\sqrt{M_0/M})_N = 5 \times 10^{-14}$. Thus, $G = G_0$ within the experimental errors and agreement with the binary pulsar data for the periastron shift is obtained for $K_N \ll 4.2 \text{ km}$.

For a massless photon $E = 0$ and we have

$$\frac{d^2 u}{d\phi^2} + u = 3 \frac{GM}{c^2} u^2. \quad (101)$$

For the solar system using (99) this gives the light deflection:

$$\Delta_{\odot} = \frac{4G_0 M_{\odot}}{c^2 R_{\odot}} \quad (102)$$

in agreement with GR.

9 Galaxy Clusters and Lensing

We can assess the existence of dark matter of galaxies and clusters of galaxies in two independent ways: from the dynamical behavior of test particles through the

study of extended rotation curves of galaxies, and from the deflection and focusing of electromagnetic radiation, e.g., gravitational lensing of clusters of galaxies. The light deflection by gravitational fields is a relativistic effect, so the second approach provides a way to test the relativistic effects of gravitation at the extra-galactic level. It has been shown that for conformal tensor-scalar gravity theories the bending of light is either the same or can even be weaker than predicted by GR [25, 28]. To remedy this problem, Bekenstein [25] has recently formulated a relativistic description of Milgrom's MOND model, including a time-like vector field as well as two scalar fields within a GR metric scenario. However, the time-like vector field violates local Lorentz invariance and requires preferred frames of reference.

The bending angle of a light ray as it passes near a massive system along an approximately straight path is given to lowest order in v^2/c^2 by

$$\theta = \frac{2}{c^2} \int |a^\perp| dz, \quad (103)$$

where \perp denotes the perpendicular component to the ray's direction, and dz is the element of length along the ray and a denotes the acceleration. The best evidence in favor of dark matter lensing is the observed luminous arcs seen in the central regions of rich galaxy clusters [29]. The cluster velocity dispersion predicted by the observed arcs is consistent within errors with the observed velocity dispersion of the cluster galaxies. This points to a consistency between the virial mass and the lensing mass, which favors the existence of dark matter.

From (101), we obtain the light deflection

$$\Delta = \frac{4GM}{c^2 R} = \frac{4G_0 \overline{M}}{c^2 R}, \quad (104)$$

where

$$\overline{M} = M \left(1 + \sqrt{\frac{M_0}{M}} \right). \quad (105)$$

We obtain from Eq.(74) and $k = 2 \times 10^{-13}$ for a mean orbital cluster radius $\langle r_{\text{orb}} \rangle_{\text{cl}} \sim 2$ Mpc:

$$\alpha_{\text{cl}} \equiv (\sqrt{M_0})_{\text{cl}} = 3.1 \times 10^{24} \text{ g}^{1/2}. \quad (106)$$

For a cluster of mass $M_{\text{cl}} \sim 10^{13} M_\odot$, we obtain

$$\left(\sqrt{\frac{M_0}{M}} \right)_{\text{cl}} \sim 22. \quad (107)$$

We see that $\overline{M} \sim 22M$ and we can explain the increase in the light bending without exotic dark matter.

From the formula Eq.(72) for $r \gg r_0 \sim 14$ kpc we get

$$a(r) = -\frac{G_0 \overline{M}}{r^2}. \quad (108)$$

We expect to obtain from this result a satisfactory description of lensing phenomena using Eq.(103).

The scaling by the parameter $\alpha_i = (\sqrt{M_0})_i$ caused by the varying strength of the coupling of the skew field $g_{[23]}(r) = f(r) \sin \theta$ to matter due to the renormalized gravitational constant is seen to play an important role in describing consistently the solar system and the galaxy and cluster dynamics, without the postulate of exotic dark matter.

10 Conclusions

There is a large enough sample of galaxy data which fits our predicted NGT acceleration law to warrant taking seriously the proposal that NGT can explain the flat rotational velocity curves of galaxies without exotic dark matter. We do predict that there will be galaxy matter additional to that due to visible stars and baryons, associated with the energy density ρ_m residing in the skew field $g_{[\mu\nu]}$. It is interesting to note that we can fit the rotational velocity data of galaxies in the distance range $0.02 \text{ kpc} < r < 70 \text{ kpc}$ and in the mass range $10^5 M_\odot < M < 10^{11} M_\odot$. without exotic dark matter halos. We are required to investigate further the behavior of the NGT predictions for distances approaching the cores of galaxies, using a disk profile density. The lensing of clusters can also be explained by the theory without exotic dark matter in cluster halos.

We are able to obtain agreement with the observations in the solar system and terrestrial gravitational experiments for suitable values of the parameter M_0 . This required that we scale G and the parameter $\sqrt{M_0}$ as functions of the mean orbital radius $\langle r_{\text{orb}} \rangle$ of bound systems with the behavior $\alpha_i = (\sqrt{M_0})_i = \langle r_{\text{orb}} \rangle_i^{3/2}$.

A numerical solution of the NGT field equations for cosmology must be implemented to see whether the theory can account for the large scale structure of the universe and account for galaxy formation and big bang nucleosynthesis, without requiring the existence of exotic, undetected dark matter and a positive cosmological constant to describe dark energy.

11 Appendix A: The Static Spherically Symmetric Solution and the Vacuum Field Equations

In the case of a spherically symmetric static field [5], the canonical form of $g_{\mu\nu}$ in NGT is given by

$$g_{\mu\nu} = \begin{pmatrix} -\alpha & 0 & 0 & w \\ 0 & -\beta & f \sin \theta & 0 \\ 0 & -f \sin \theta & -\beta \sin^2 \theta & 0 \\ -w & 0 & 0 & \gamma \end{pmatrix}, \quad (109)$$

where α, β, γ and w are functions of r . The tensor $g^{\mu\nu}$ has the components:

$$g^{\mu\nu} = \begin{pmatrix} \frac{\gamma}{w^2 - \alpha\gamma} & 0 & 0 & \frac{w}{w^2 - \alpha\gamma} \\ 0 & -\frac{\beta}{\beta^2 + f^2} & \frac{f \csc \theta}{\beta^2 + f^2} & 0 \\ 0 & -\frac{f \csc \theta}{\beta^2 + f^2} & -\frac{\beta \csc^2 \theta}{\beta^2 + f^2} & 0 \\ -\frac{w}{w^2 - \alpha\gamma} & 0 & 0 & -\frac{\alpha}{w^2 - \alpha\gamma} \end{pmatrix}. \quad (110)$$

For the theory in which there is no NGT magnetic monopole charge, we have $w = 0$ and only the $g_{[23]}$ component of $g_{[\mu\nu]}$ survives.

The time independent field equations, Eq.(21), in empty space are given by

$$R_{11}(\Gamma) = -\frac{1}{2}A'' - \frac{1}{8}[(A')^2 + 4B^2] + \frac{\alpha'A'}{4\alpha} + \frac{\gamma'}{2\gamma} \left(\frac{\alpha'}{2\alpha} - \frac{\gamma'}{2\gamma} \right) \quad (111)$$

$$-\left(\frac{\gamma'}{2\gamma} \right)' = -\Lambda\alpha + \frac{1}{4}\mu^2 \frac{\alpha f^2}{\beta^2 + f^2}, \quad (112)$$

$$\frac{1}{\beta}R_{22}(\Gamma) = \frac{1}{\beta}R_{33}(\Gamma)\operatorname{cosec}^2\theta = \frac{1}{\beta} + \frac{1}{\beta} \left(\frac{2fB - \beta A'}{4\alpha} \right)' + \frac{2fB - \beta A'}{8\alpha^2\beta\gamma} (\alpha'\gamma + \gamma'\alpha) \quad (113)$$

$$+ \frac{B(fA' + 2\beta B)}{4\alpha\beta} = -\Lambda - \frac{1}{4}\mu^2 \frac{f^2}{\beta^2 + f^2}, \quad (114)$$

$$R_{00}(\Gamma) = \left(\frac{\gamma'}{2\alpha} \right)' + \frac{\gamma'}{2\alpha} \left(\frac{\alpha'}{2\alpha} - \frac{\gamma'}{2\gamma} + \frac{1}{2}A' \right) = \Lambda\gamma - \frac{1}{4}\mu^2 \frac{\gamma f^2}{\beta^2 + f^2}, \quad (115)$$

$$R_{[10]}(\Gamma) = 0, \quad (116)$$

$$R_{(10)}(\Gamma) = 0, \quad (117)$$

$$R_{[23]}(\Gamma) = \sin\theta \left[\left(\frac{fA' + 2\beta B}{4\alpha} \right)' + \frac{1}{8\alpha} (fA' + 2\beta B) \left(\frac{\alpha'}{\alpha} + \frac{\gamma'}{\gamma} \right) \right] \quad (118)$$

$$- \frac{B}{4\alpha} (2fB - \beta A') = \left[\Lambda f - \frac{1}{4}\mu^2 f \left(1 + \frac{\beta^2}{\beta^2 + f^2} \right) \right] \sin\theta. \quad (119)$$

Here, prime denotes differentiation with respect to r , and we have used the notation

$$A = \ln(\beta^2 + f^2), \quad (120)$$

$$B = \frac{f\beta' - \beta f'}{\beta^2 + f^2}. \quad (121)$$

Let us assume the long-range approximation for which the μ^2 contributions in the vacuum field equations (21) can be neglected and that $\mu^{-1} > 2M$. We then obtain the static, spherically symmetric Wyman solution for $\Lambda = 0$ [9]:

$$\gamma = \exp(\nu), \quad (122)$$

$$\alpha = \frac{(f^2 + \beta^2)(\gamma')^2}{4M_1^2\gamma}, \quad (123)$$

$$f + i\beta = \frac{M_1^2(1 + is) \exp(-\nu)}{A + i} \operatorname{sech}^2\left[-\frac{1}{2}(1 + is)^{1/2}\nu + B\right], \quad (124)$$

where M_1, A, B and s are integration constants and ν is an arbitrary function of r .

We shall restrict our attention to the asymptotic condition $g_{(\mu\nu)} \rightarrow \eta_{\mu\nu}$ where $\eta_{\mu\nu}$ is the Minkowski flat metric tensor $\eta_{\mu\nu} = \operatorname{diag}(1, -1, -1, -1)$. This requires that

$$\sinh^2 B = -1, \quad (125)$$

so that we obtain

$$f + i\beta = -\frac{M_1^2(1 + is) \exp(-\nu)}{A + i} \operatorname{csch}^2\left[-\frac{1}{2}(1 + is)^{1/2}\nu\right]. \quad (126)$$

This form of $f + i\beta$ does not place any *a priori* boundary condition on $g_{[\mu\nu]}$.

We now obtain the form of the static Wyman solution:

$$\gamma = \exp(\nu), \quad (127)$$

$$\alpha = \frac{M_1^2(\nu')^2 \exp(-\nu)(1 + s^2)}{A + i} [\cosh(a\nu) - \cos(b\nu)]^{-2}, \quad (128)$$

$$\begin{aligned} f &= \frac{2M_1^2}{1 + A^2} \exp(-\nu) [(1 - As) \sinh(a\nu) \sin(b\nu) \\ &+ s(1 - \cosh(a\nu) \cos(b\nu))] [\cosh(a\nu) - \cos(b\nu)]^{-2}, \end{aligned} \quad (129)$$

where

$$a = \left(\frac{\sqrt{1 + s^2} + 1}{2}\right)^{1/2}, \quad b = \left(\frac{\sqrt{1 + s^2} - 1}{2}\right)^{1/2}, \quad (130)$$

and ν is implicitly determined by the equation

$$\begin{aligned} \exp(\nu) (\cosh(a\nu) - \cos(b\nu))^2 \frac{r^2(1 + A^2)}{2M_1^2} &= (1 - As) [\cosh(a\nu) \cos(b\nu) - 1] \\ &+ (A + s) \sinh(a\nu) \sin(b\nu). \end{aligned} \quad (131)$$

At large distances $r \rightarrow \infty$, we have

$$\alpha = 1 + \frac{2M_1}{(1 + A^2)^{1/2}} \frac{1}{r} + O\left(\frac{1}{r^2}\right), \quad (132)$$

$$\gamma = 1 - \frac{2M_1}{(1 + A^2)^{1/2}} \frac{1}{r} + O\left(\frac{1}{r^3}\right), \quad (133)$$

$$f = -Ar^2 + \frac{1}{3}sM_1^2 + O\left(\frac{1}{r}\right). \quad (134)$$

If we assume that $A = 0$, then $M = M_1$ where M denotes the mass of the particle source.

Acknowledgments

This work was supported by the Natural Sciences and Engineering Research Council of Canada. I thank Hilary Carteret for help with the use of Maple 9 software and Gilles Esposito-Farèse, Gary Mamon, Stacey McGough, Martin Green and Lee Smolin for helpful discussions.

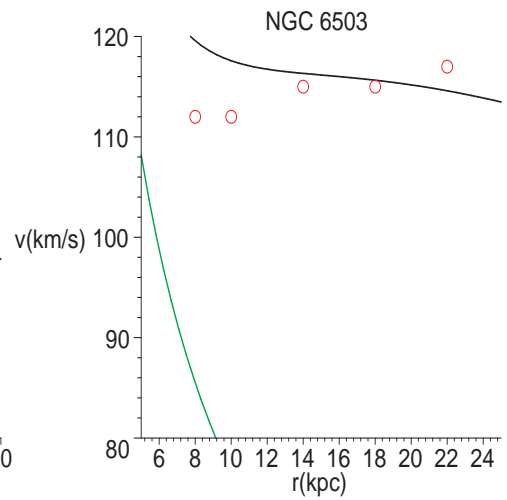
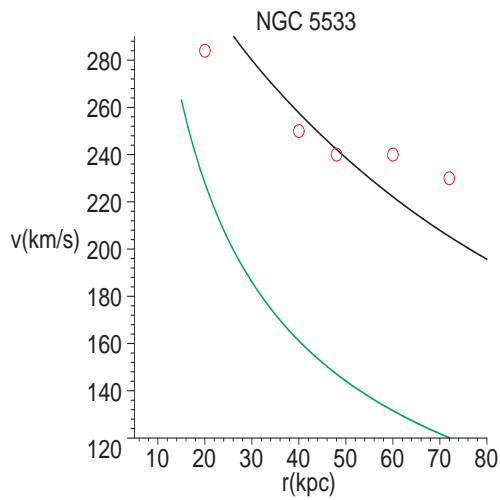
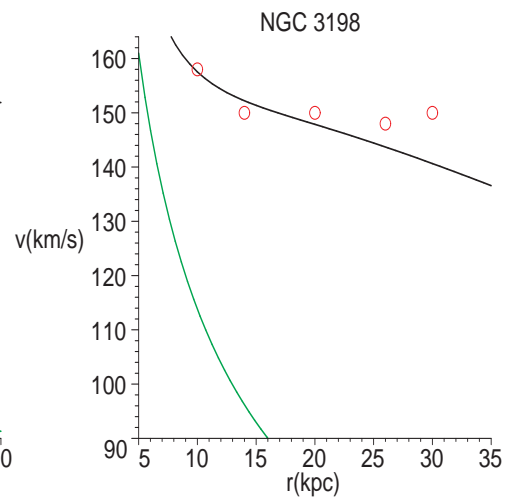
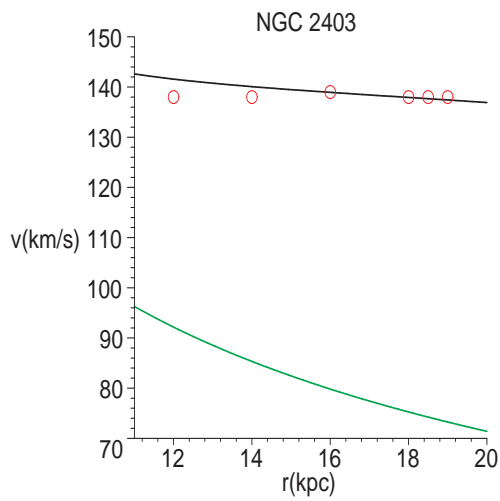
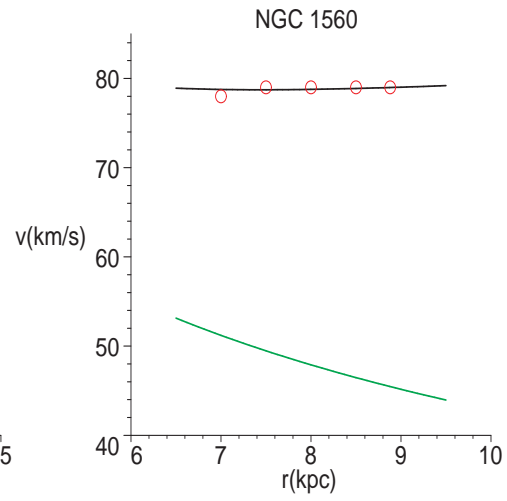
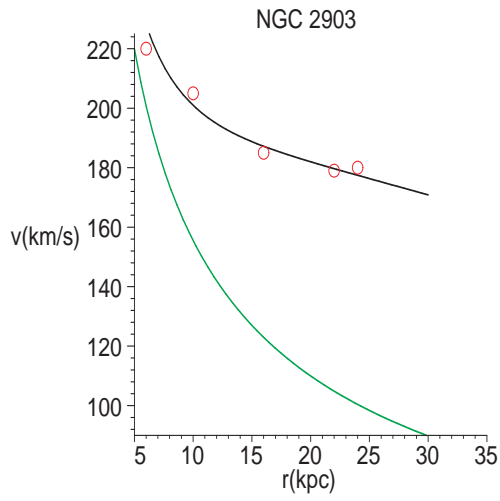
References

- [1] S. Perlmutter et al. *Ap. J.* **483**, 565 (1997), astro-ph/9608192; A. G. Riess, et al. *Astron. J.* **116**, 1009 (1998), astro-ph/9805201; P. M. Garnavich, et al. *Ap. J.* **509**, 74 (1998), astro-ph/9806396.
- [2] A. G. Riess, et al. astro-ph/0402512.
- [3] D. N. Spergel et al. *Astrophys. J. Suppl.* **148**, 175 (2003), astro-ph/0302209.
- [4] J. W. Moffat, astro-ph/0403266.
- [5] J. W. Moffat, *Phys. Rev.* **19**, 3554 (1979).
- [6] J. W. Moffat, *Phys. Letts. B* **335**, 447 (1995), gr-qc/9411006.
- [7] J. W. Moffat, *J. Math. Phys.* **36**, 3722 (1995); Erratum, *J. Math. Phys.* **36**, 7128 (1995).
- [8] S. Weinberg, *Rev. Mod. Phys.* **61**, 1 (1989); N. Straumann, astro-ph/020333.
- [9] M. Wyman, *Can J. Math.* **2**, 427 (1950); J. R. Vanstone, *Can J. Math.* **14**, 568 (1962).
- [10] J. Légaré and J. W. Moffat, *Gen. Rel. and Grav.* **28**, 1221 (1996), gr-qc/9509035; J. Légaré and J. W. Moffat, gr-qc/9412074.
- [11] J. Légaré and J. W. Moffat, *Gen. Rel. and Grav.* **27**, 761 (1995), gr-qc/9412009.
- [12] A. Papapetrou, *Lectures on General Relativity* (Reidel, Dordrecht) (1978).
- [13] M. Kalb and P. Ramond, *Phys. Rev.* **D9**, 2273 (1974).
- [14] M. A. Clayton, *J. Math. Phys.* **37**, 395 (1996), gr-qc/9505005.
- [15] N. J. Cornish, PhD Thesis, University of Toronto, Toronto, Canada 1996.
- [16] J. W. Moffat and I. Yu. Sokolov, *Phys. Lett.* **B378**, 59 (1996), astro-ph/9509143.

- [17] <http://pdg.lbl.gov>.
- [18] R. H. Sanders and S. S. McGaugh, *Ann. Rev. Astron. Astrophys.* **40**, 263 (2002), astro-ph/0204521.
- [19] R. B. Tully and J. R. Fisher, *Astr. Ap.* **54**, 661 (1977).
- [20] E. L. Lokas, *Mon. Not. R. Astron. Soc.* **333**, 697 (2002), astro-ph/0112023.
- [21] M. Mateo, *Ann. Rev. Astron. Astrophys.* **36**, 435 (1998).
- [22] J. Kormendy and K. C. Freeman, *Dark Matter in Galaxies*, Proceedings of the IAU Symposium No. 220, 2004 IAU, eds. S. Ryder, D. J. Pisano, M. Walker and K. C. Freedman, San Francisco: ASP, 2004, astro-ph/0407321.
- [23] A. J. Romanowsky et al. , Science Express Reports, 28 August, 2003, astro-ph/0308518; A. J. Romanowsky et al. *Dark matter in Galaxies*, Proc. IAU Symposium No. 220, eds. S. Ryder, D. J. Pisano, M. Walker and K. Freedman, San Francisco: ASP, 2004, astro-ph/0310874.
- [24] M. Milgrom, *Ap. J.* **270**, 365 (1983).
- [25] J. D. Bekenstein, astro-ph/0403694.
- [26] M. Milgrom and R. H. Sanders, *Astrophys. J.* **599**, L25 (2003), astro-ph/0309617.
- [27] D. E. McLaughlin and G. Meylan, *New Horizons in Globular Cluster Astronomy* ASP Conference Series, 2003, eds. G. Piotto, G. Meylan. G. Djorgovski and M. Riello.
- [28] J. D. Bekenstein and R. H. Sanders, *Ap. J.* **429**, 480 (1994), astro-ph/9311062.
- [29] R. D. Blanford and R. Narayan, *Ann. Rev. Astron. Astrophys.* **30**, 311 1992.

Table 1. Values of the total galaxy mass M used to fit rotational velocity data. Also shown are the mass-to-light-ratios M/L with L obtained from ref. [18].

Galaxy	$M(\times 10^{10} M_{\odot})$	$M/L(M_{\odot}/L_{\odot})$
NGC 2903	5.63	3.68
NGC 5533	24.2	4.29
NGC 5907	11.8	4.92
NGC 6503	1.36	2.84
NGC 3198	3.0	3.33
NGC 2403	2.37	3.0
NGC 1560	0.427	12.20
NGC 4138	2.94	3.59
NGC 3379	5.78	–
M33	0.93	1.98
UGC 6917	0.96	2.53
UGC 6923	0.388	1.76
UGC 6930	1.04	2.08
FORNAX	0.0026	1.86
DRACO	0.00050	27.94
ω Centauri	3.05×10^{-5}	–



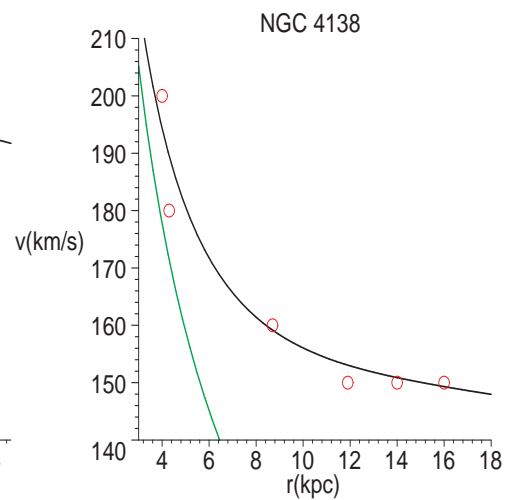
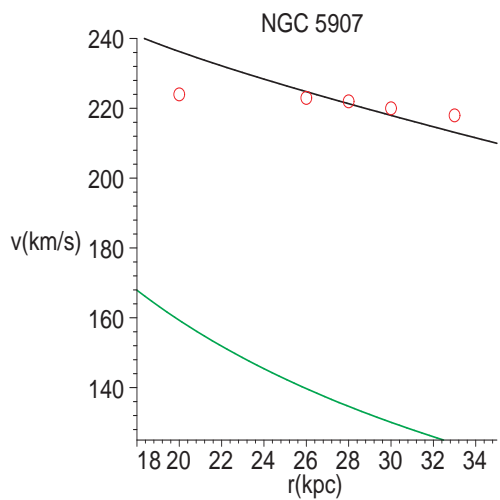
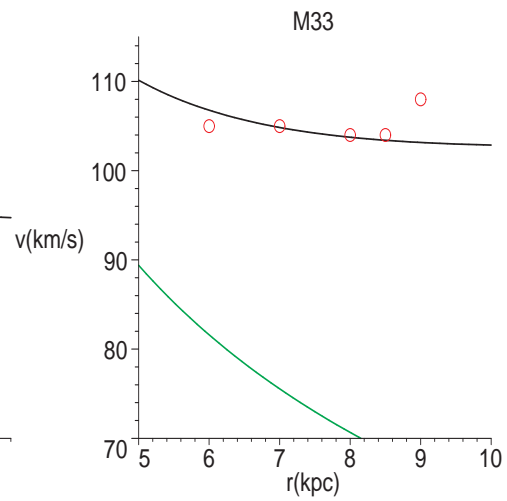
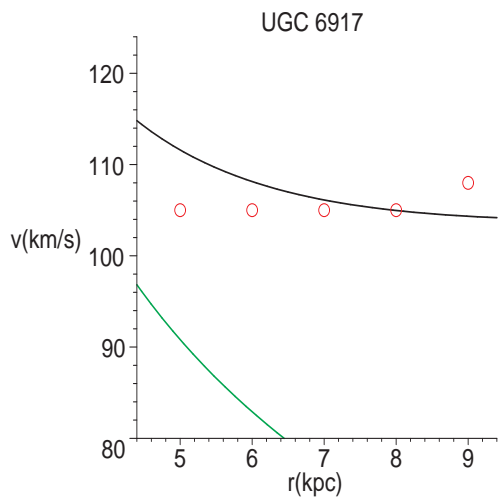
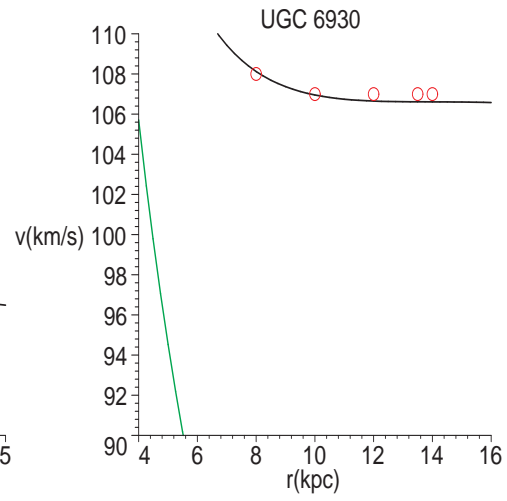
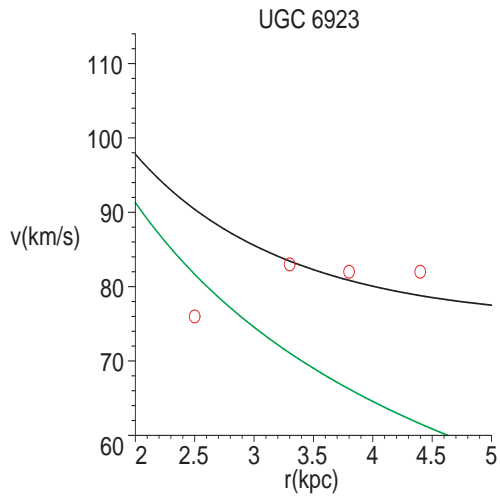


Fig. 1 - Fits to low-surface-brightness and high-surface-brightness spiral galaxy data. The black curve is the rotational velocity v versus r obtained from the modified Newtonian acceleration, while the green curve shows the Newtonian rotational velocity v versus r . The data are shown as red circles.

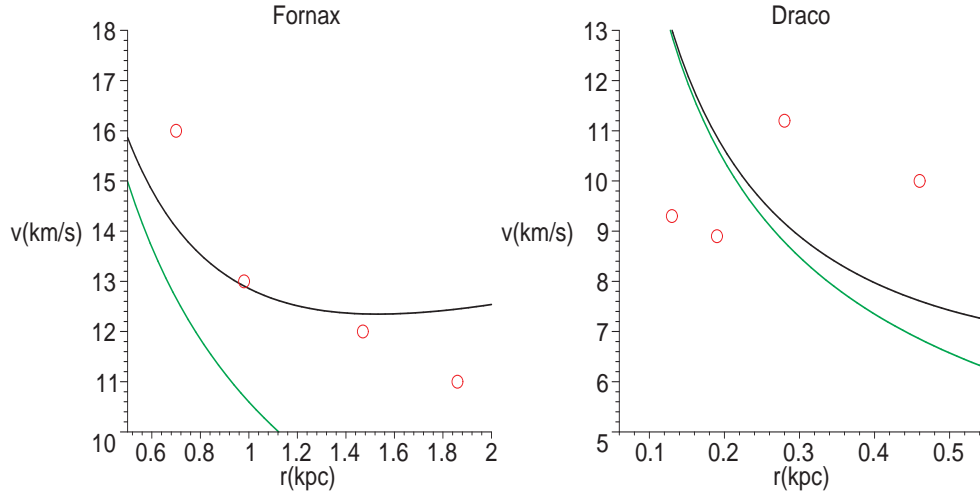


Fig. 2 - Fits to the data of two dwarf galaxies Fornax and Draco. The simple relation $V \sim \sqrt{2}\sigma$ is assumed between the velocity dispersion σ and the rotational velocity v . The black curve is the rotational velocity v versus r obtained from the modified Newtonian acceleration, while the green curve shows the Newtonian rotational velocity v versus r . The data are shown as red circles and the errors (not shown) are large and for Draco the Newtonian fit cannot be distinguished from the NGT fit to the data within the errors.

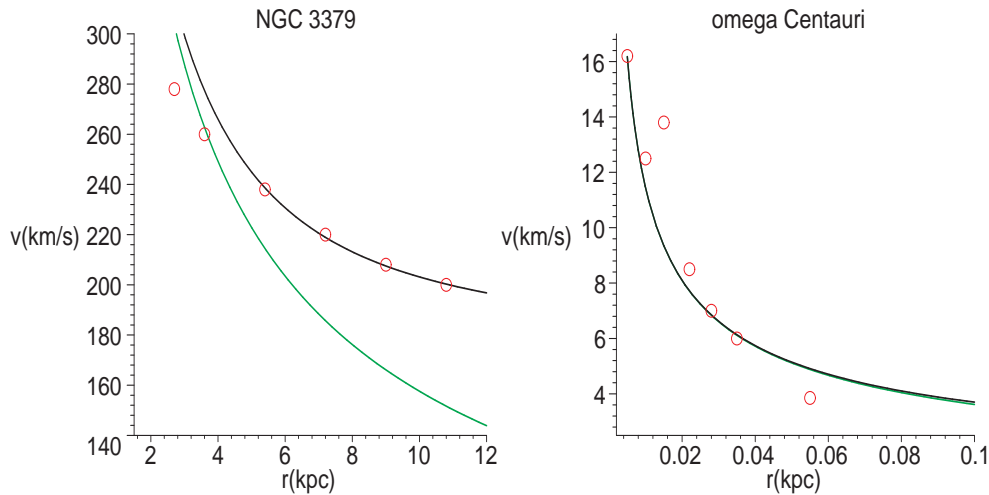


Fig. 3 - Fits to the elliptical galaxy NGC 3379 and the globular cluster ω Centauri. The black curve is the rotational velocity v versus r obtained from the modified NGT acceleration, while the green curve is the Newtonian-Kepler velocity curve. For ω Centauri the black and green curves cannot be distinguished from one another.

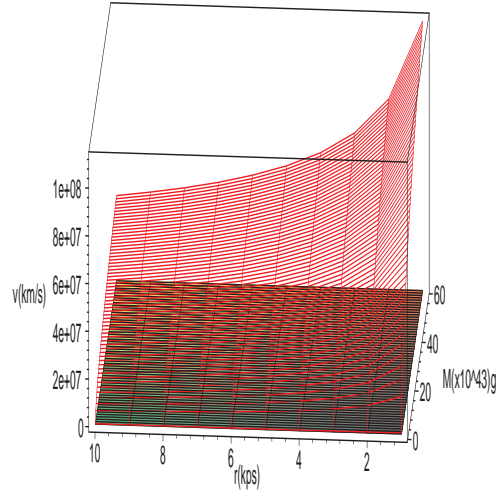


Fig. 4 - 3-dimensional plot of v versus the range of distance $0.1 \text{ kpc} < r < 10 \text{ kpc}$ and the range of galaxy mass $5 \times 10^6 M_{\odot} < M < 2.5 \times 10^{11} M_{\odot}$. The red surface shows the Newtonian values of the rotational velocity v , while the black surface displays the NGT prediction for v .